Journal of Cellular Biochemistry 102:1458–1471 (2007)

Identification of Novel Runx2 Targets in Osteoblasts: Cell Type-Specific BMP-Dependent Regulation of Tram2

Steven Pregizer,[1] Artem Barski,[1] Charles A. Gersbach,[2,3] Andrés J. García,[3,4] and Baruch Frenkel[1,5]*

[1]Department of Biochemistry & Molecular Biology, Institute for Genetic Medicine, Keck School of Medicine at the University of Southern California, Los Angeles, California 90033
[2]Coulter Department of Biomedical Engineering, Georgia Institute of Technology and Emory University, Atlanta, Georgia 30332
[3]Georgia Tech/Emory Center for the Engineering of Living Tissues, Georgia Institute of Technology, Atlanta, Georgia 30332
[4]Woodruff School of Mechanical Engineering, Georgia Institute of Technology, Atlanta, Georgia 30332
[5]Department of Orthopedic Surgery, University of Southern California, Los Angeles, California 90033

Abstract Runx2 is an osteoblast master transcription factor and a target for bone morphogenetic protein (BMP) signaling, but our knowledge of events downstream of Runx2 is limited. In this study, we used ChIP Display to discover seven novel genomic regions occupied by Runx2 in living MC3T3-E1 osteoblastic cells. Six of these regions are found within or up to 1-kb away from annotated genes, but only two are found within 5′-gene flanking sequences. One of the newly identified Runx2 target genes is Tram2, whose product facilitates proper folding of type I collagen. We demonstrate that Tram2 mRNA is suppressed in non-osteoblasts when Runx2 is over-expressed, and that this suppression is alleviated upon treatment with BMP-2. Moreover, we show that BMP-induced Runx2 expression in the C3H10T1/2, ST2, C2C12, and MC3T3-E1 cell lines coincides with an increase in Tram2 mRNA levels. Thus, Runx2 may regulate Tram2 expression in a BMP-dependent manner, and Tram2 may participate in the overall osteogenic function of Runx2. Among the other Runx2 target genes discovered in this study are Lnx2, an intracellular scaffolding protein that may play a role in Notch signaling, and Tnfrsf12a, a Tumor Necrosis Factor receptor family member that influences both osteoblast and osteoclast differentiation. Expanding our knowledge of Runx2 target genes, and manipulation of these genes, are warranted to better understand the regulation of osteoblast function and to provide opportunities for the development of new bone anabolics. J. Cell. Biochem. 102: 1458–1471, 2007.

Key words: Runx2; ChIP display; Tram2; osteoblast; location analysis

Runx2 is important for skeletal development and homeostasis. In humans, Runx2 polymorphisms are associated with variations in bone mineral density, while heterozygous mutations cause cleidocranial dysplasia (CCD) [Mundlos et al., 1997; Vaughan et al., 2002, 2004; Doecke et al., 2006]. Heterozygous Runx2 mutant mice recapitulate the CCD phenotype, while homozygotes have skeletons that fail to mineralize, owing to a complete arrest in osteoblast differentiation [Komori et al., 1997; Otto et al., 1997]. Mice expressing dominant negative Runx2 under the control of the osteocalcin promoter have osteopenia, as do those expressing wild-type Runx2 under the control of the type I collagen promoter. The former is due to compromised osteoblast function [Ducy et al., 1999], whereas the latter is due to a late-stage maturational block in osteoblast differentiation [Liu et al., 2001; Geoffroy et al., 2002]. In each of these cases, the consequence of interfering with endogenous Runx2 is a defect in normal osteoblast development or function, resulting in a severely compromised skeleton. Thus, an important task in skeletal biology is to better

Grant sponsor: NIH; Grant numbers: DK071122, EB003364, T 32 GM067587, RR10600-01, CA62528-01, RR14514-01.

*Correspondence to: Baruch Frenkel, Institute for Genetic Medicine, University of Southern California Keck School of Medicine, 2250 Alcazar Street, CSC/IGM240, Los Angeles, CA 90033. E-mail: frenkel@usc.edu

Received 25 January 2007; Accepted 12 March 2007

DOI 10.1002/jcb.21366

define the role of Runx2 by studying its regulation and mechanism of action in osteoblasts.

It is well established that Runx2 can regulate the transcription of genes in osteoblasts by binding to sequences resembling the 5′-ACACCA-3′ motif some distance upstream from their transcription start sites. Activation of transcription in this manner has been demonstrated for osteocalcin, bone sialoprotein, osteopontin, type I collagen, fibronectin, galectin 3, MMP13, and OPG [Banerjee et al., 1997; Ducy et al., 1997; Sato et al., 1998b; Harada et al., 1999; Xiao et al., 1999; Lee et al., 2000; Kern et al., 2001; Prince et al., 2001]. It is tempting to conclude that the dramatic role of Runx2 in skeletal biology is mediated by these genes; however, genetic knock-out studies in mice suggest that each of bone sialoprotein, osteocalcin, osteopontin, OPG, galectin-3, and MMP13 is unnecessary for osteoblast differentiation and function [Aubin et al., 1996; Ducy et al., 1996; Bucay et al., 1998; Colnot et al., 1998; Mizuno et al., 1998; Rittling et al., 1998; Inada et al., 2004; Stickens et al., 2004]. Type I collagen is necessary, but not sufficient for skeletogenesis [Murshed et al., 2005]. In view of these findings, it is reasonable to assume that unknown Runx2 target genes exist, which mediate its pivotal role in skeletal biology.

The few known Runx2 target genes have been typically identified based on a candidate approach. Promoters of genes with established roles in osteoblast biology were screened for Runx2 cognate sites, and the functionality of these sites was confirmed by protein-DNA interaction and transcription assays [Sato et al., 1998a; Jimenez et al., 1999; Thirunavukkarasu et al., 2000; Javed et al., 2001; Kern et al., 2001; Stock et al., 2003]. Obviously, such approaches cannot yield novel Runx2 target genes. Two groups have used microarrays to identify novel Runx2-regulated genes based their differential expression in cells from $Runx2^{-/-}$ versus wild type mice [Vaes et al., 2006; Hecht et al., 2007]. While this approach dramatically increases the number of candidates, it is limited to those genes spotted on the array. Moreover, expression microarray studies are fraught with reproducibility and sensitivity problems [Irizarry et al., 2005].

Whether a candidate Runx2 target gene emerges from archival bone literature or from contemporary comprehensive gene expression profiling, and even if the candidate is a direct Runx2 target, a question that cannot be effectively addressed based on expression studies is the location of *cis*-acting elements responsible for the regulation by Runx2. Traditionally, investigators searching for Runx2-binding elements have focused on 5′-flanking sequences [Sato et al., 1998a; Jimenez et al., 1999; Thirunavukkarasu et al., 2000; Javed et al., 2001; Kern et al., 2001; Stock et al., 2003]; however, there is a growing body of evidence suggesting that transcription factors bind to other regions as well [Cawley et al., 2004; Loh et al., 2006]. The task of mapping regulatory sequences that mediate Runx2 action on target genes is further complicated by the fact that the Runx2 consensus motif is only 6-bp long and quite promiscuous, resulting in a large number of putative binding sites, which greatly exceed the number of functional sites [Roca et al., 2005]. Furthermore, sequences to which Runx2 binds in living cells may be different from the consensus, which was defined in vitro [Meyers et al., 1993], and, Runx2 may even be recruited to DNA indirectly via interaction with other transcription factors.

The search for transcription factor targets has been propelled in recent years by the development of a group of novel techniques, collectively known as location analysis. Location analysis is based on the physical interaction of transcription factors with their target genomic loci, and thus does not suffer from the aforementioned drawbacks. Furthermore, location analysis can discover target genes for transcription factors even when regulation of these genes by the transcription factor of interest occurs under conditions that are difficult to model experimentally.

Location analysis is based on chromatin immunoprecipitation (ChIP), which has been used traditionally to test whether a candidate DNA fragment is occupied by a transcription factor of interest in living cells. Because ChIP concentrates all DNA fragments occupied by the transcription factor of interest, it can be modified to discover novel binding regions. The simplest approach to this is cloning and sequencing of the ChIP products. Unfortunately, ChIP-cloning is rather tedious and yields a high false positive rate, due to the high amount of non-specifically immunoprecipitated DNA [Weinmann et al., 2001]. Approaches that are more high-throughput and have lower false positive rates include Serial Analysis of Binding

Elements (SABE) [Chen and Sadowski, 2005], Sequence Tag Analysis of Genomic Enrichment (STAGE) [Kim et al., 2005], Paired-End Ditag Sequencing (ChIP-PET) [Wei et al., 2006], Genome-Wide Mapping Technique (GMAT) [Roh et al., 2004], Serial Analysis of Chromatin Occupancy (SACO) [Impey et al., 2004], and ChIP-chip [Ren et al., 2000; Horak and Snyder, 2002; Cawley et al., 2004]. The major drawbacks to these approaches are that they require large amounts of starting material, complicated statistical analysis, and financial resources unavailable to the average molecular biology laboratory. One approach that is less high-throughput, but does not suffer from the aforementioned limitations is ChIP Display (CD). We demonstrated in a pilot study that CD can discover novel targets of Runx2 in osteoblasts [Barski and Frenkel, 2004]. In this study, we used CD to discover additional targets, and focused on one, Tram2, which likely participates in the execution of Runx2's role in osteoblasts.

MATERIALS AND METHODS

Cell Culture

A subclone derived from the MC3T3-E1 osteoblastic cell line was used for ChIP assay and CD [Smith et al., 2000]. Cells were maintained in α-MEM supplemented with 10% fetal bovine serum (FBS) (Invitrogen). Starting at confluence, 10 mM sodium β-glycerophosphate and 50 μg/ml ascorbic acid (Sigma) were added to support differentiation. ST2 cells (Riken) were maintained in RPMI1640 supplemented with 10% FBS, while C3H10T1/2 and C2C12 cells were maintained in DMEM supplemented with 10% FBS. Primary skeletal myoblasts were cultured as previously described [Gersbach et al., 2006]. When indicated, 300 ng/ml recombinant human BMP-2 (rhBMP-2) was added starting at confluence and at each subsequent feeding.

ChIP Display

CD was performed essentially as previously described [Barski and Frenkel, 2004]. This method entails the resolution of the DNA from Runx2 chromatin immunoprecipitates by polyacrylamide gel electrophoresis after *Ava*II digestion, linker ligation, and PCR amplification [Barski and Frenkel, 2004]. To reduce the complexity of products that are seen on a gel, the ligated restriction fragments are amplified in 36 separate reactions with 8 nested PCR primers (Table I), alone or pair-wise [Barski and Frenkel, 2004]. Each PCR primer contains either an A or a T at the +3 position of the *Ava*II site and an A, T, G, or C at the position immediately internal to the *Ava*II site (+6). Primers are named according to the nucleotides occupying these positions; for example, the 'AG' primer has an A at position +3 and G at position +6. Bands of interest are excised from the polyacrylamide gel, reamplified and subjected

TABLE I. Oligonucleotides Used in This Study

Name	Sequence
Short CD linker	5′-TTC GCG GCC GCA C-3′
Long CD *A* linker	5′-GAC GTG CGG CCG CGA A-3′
Long CD *T* linker	5′-GTC GTG CGG CCG CGA A-3′
"AA" CD primer	5′-CGG CCG CAC GAC CA-3′
"AT" CD primer	5′-CGG CCG CAC GAC CT-3′
"AG" CD primer	5′-CGG CCG CAC GAC CG-3′
"AC" CD primer	5′-CGG CCG CAC GAC CC-3′
"TA" CD primer	5′-CGG CCG CAC GTC CA-3′
"TT" CD primer	5′-CGG CCG CAC GTC CT-3′
"TG" CD primer	5′-CGG CCG CAC GTC CG-3′
"TC" CD primer	5′-CGG CCG CAC GTC CC-3′
Tram2 forward ChIP primer	5′-AGC TCT GCA ATT GGT TCG-3′
Tram2 reverse ChIP primer	5′-TGT CCC GCA CGT TAT CTG-3′
Insulin forward ChIP primer	5′-AAC TGG TTC ATC AGG CCA TCT GGT C-3′
Insulin reverse ChIP primer	5′-TGG ATG CCC ACC AGC TTT ATA GTC C-3′
Osteocalcin forward ChIP primer	5′-GAG AGC ACA CAG TAG GAG TGG TGG AG-3′
Osteocalcin reverse ChIP primer	5′-TCC AGC ATC CAG TAG CAT TTA TAT CG-3′
L10A forward qRT-PCR primer	5′-CGC CGC AAG TTT CTG GAG AC-3′
L10A reverse qRT-PCR primer	5′-CTT GCC AGC CTT GTT TAG GC-3′
Runx2 forward qRT-PCR primer	5′-AGC CTC TTC AGC GCA GTG AC-3′
Runx2 reverse qRT-PCR primer	5′-CTG GTG CTC GGA TCC CAA-3′
Osteocalcin forward qRT-PCR primer	5′-CGG CCC TGA GTC TGA CAA A-3′
Osteocalcin reverse qRT-PCR primer	5′-GCC GGA GTC TGT TCA CTA CCT T-3′
Tram2 forward qRT-PCR primer	5′-CCC CGA GAA AGG GAA CTT TA-3′
Tram2 reverse qRT-PCR primer	5′-TTC TCT GCC TTC ACC ACT CC-3′

to secondary digestion. They are identified based on sequencing of a sub-fragment eluted after agarose gel electrophoresis.

Several modifications to CD were introduced in the present study. First, we performed the amplification of each ChIP sample in duplicate, with a 1°C difference in annealing temperature (Fig. 1A). Second, bands excised from the acrylamide gels were amplified for secondary digestion either, as originally described [Barski and Frenkel, 2004], with the primer pair used to generate the original product, or, in some cases, re-amplification was achieved with a single primer (see Fig. 1B). When the PCR was successful with a single primer, sub-fragments obtained after secondary digestion of this single-primer PCR product were used for sequencing, because they typically had less background (Fig. 1C).

Runx2 Over-Expression

Runx2 was ectopically expressed in primary myoblasts by viral infection as previously described [Gersbach et al., 2006]. C3H10T1/2 cells were transiently transfected using Lipofectamine 2000 (Invitrogen) with the Runx2 vector pCMV-Osf [Ducy et al., 1997], or the molar equivalent of pcDNA3 (Invitrogen). pCAT (Promega) was used to equalize the total amount of DNA that was transfected.

RT-PCR

RNA was collected from cells using the Aurum Total RNA Mini Kit (BioRad). One microgram of this was used to generate cDNA with the SuperScript III cDNA synthesis kit (Invitrogen). Two microliters of cDNA was used for real-time PCR with iQ^{TM} SYBR Green Supermix (BioRad). Real-time PCR was performed on an iCycler (BioRad) with MyiQ single-color detection system.

Statistical Analysis

Results from each quantitative assay were analyzed by Student's t-test to ascertain the effect of Runx2 over-expression and/or rhBMP-2 treatment on gene expression. Differences were considered significant when $P \leq 0.05$.

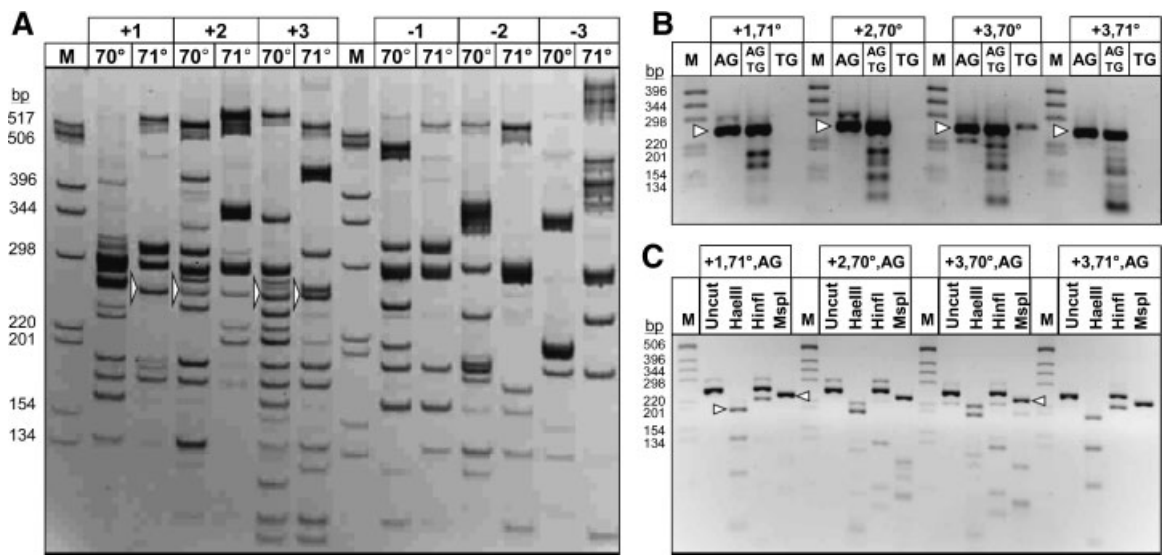

Fig. 1. Representative ChIP Display results. **A**: DNA was obtained from three Runx2 ChIPs (indicated *+1, +2, +3*) and three IgG control precipitates (*−1, −2, −3*), and amplified using various combinations of eight nested primers [Barski and Frenkel, 2004]. Products were displayed on 8% polyacrylamide gels. The one presented here shows the results obtained with the AG/TG primer pair (see Materials and Methods). Each PCR was performed with 70°C or 71°C as the annealing temperature, as indicated. Bands that appeared reproducible and specific for the Runx2 ChIPs (*arrowheads*) were excised for identification. **B**: The excised bands from **Panel A** were reamplified with the *AG*/*TG* primer pair used to generate the original product. In this experiment, each of the *AG* and *TG* primers was also employed individually, as indicated. Electrophoresis in 4% agarose gels shows that reamplification was achieved with the *AG*/*TG* primer pair, and with the *AG* primer alone, but not with the *TG* primer. Bands indicated by arrowheads were excised and eluted from the gel. **C**: The excised bands from **Panel B** were subjected to secondary digestion with the indicated restriction enzymes and were then resolved by 4% agarose gel electrophoresis. The subfragments indicated by arrowheads were purified from the gel. Direct sequencing of these subfragments was performed using the AG PCR primer. The sequence mapped to the mouse Tram2 gene. Sizes of DNA markers (*M*) are indicated in base pairs.

RESULTS

ChIP Display Discloses Novel Runx2 Genomic Targets in Living Osteoblasts

To discover novel Runx2 targets in osteoblasts, we employed ChIP Display (CD) of MC3T3-E1 osteoblastic cells [Barski and Frenkel, 2004]. While our initial Runx2 CD screen consisted of the 8 reactions that each utilize a single PCR primer, we employed in the present study all primer combinations. Furthermore, we have now performed each PCR reaction at two annealing temperatures (see Materials and Methods). An example of the results obtained with one primer pair, (the *AG* and the *TG* primers) is shown in Figure 1.

Table II depicts the position of seven Runx2-occupied regions discovered in this study and the nearby genes. Runx2 occupancy at each of these regions was confirmed by conventional ChIP assay using locus-specific primers in at least one independent experiment (see Fig. 2 for example). Six of the newly discovered Runx2 targets are found within 1 kb of known genes. These include: (i) Tram2, which has been implicated in collagen biosynthesis [Stefanovic et al., 2004]; (ii) Lnx2, a potential modulator of Notch signaling [Rice et al., 2001]; (iii) Tnfrsf12a, encoding a member of the TNF receptor superfamily [Wiley and Winkles, 2003]; (iv) Abcc8, which encodes the regulating subunit of the K^{+}_{ATP} channel [Bryan et al., 2007]; (v) Amdhd2, which contains a predicted amidohydrolase domain (www.ensembl.org); and (vi) Gm1082, a gene whose protein product has not yet been characterized. One of the seven Runx2-occupied regions was found over 50 kb from the nearest annotated transcript, which happens to be a non-coding RNA (Table II).

Interestingly, only three of those fragments found near known genes are positioned in the vicinity of the respective transcription start site (Table II). One of these encompasses the exon1/intron1 boundary of Tram2 (Fig. 2A), a gene necessary for proper synthesis and secretion of collagen type I [Stefanovic et al., 2004]. As depicted in Figure 2A, a perfect Runx2 consensus motif is present 210-bp downstream of the *Ava*II restriction fragment, which was excised from the CD acrylamide gel (Fig. 1A). The conventional ChIP assay to confirm Runx2 occupancy at the Tram2 locus was performed using primers flanking the Runx2 motif (Fig. 2B). The rationale for this design is that fragments generated during ChIP are in the order of 500–1,000 bps; thus, precipitation of the 243-bp *Ava*II fragment likely occurred due to binding of Runx2 to its adjacent cognate motif, not to any sequence within the 243-bp *Ava*II fragment [Barski et al., 2004]. Be that as it may, the robust signal obtained in the conventional ChIP assay (Fig. 2B) leaves no doubt that Runx2 occupies this locus, although, like any ChIP assay, it does not allow precise mapping. Given the role of Tram2 in collagen synthesis, and since collagen type I is the most abundant organic component of the bone extracellular matrix, we hypothesized that Runx2 might be positively regulating *Tram2* expression.

Runx2 Inhibits Tram2 Expression in Non-Osteoblasts

The role of Runx2 in the regulation of Tram2 gene expression was initially addressed using

TABLE II. Runx2-Occupied Genomic Sites Disclosed in the Present Study

Primer pair[a]	Chromosome no. and (absolute position)[b]	Nearest annotated transcript	Positional relationship to nearest gene
TG, AG	1 (21064103–346)	Translocating chain-associating membrane protein 2 (Tram2)	Straddles boundary between first exon and intron
TC, TT	5 (147386706–7208)	Ligand of numb-protein X 2 (Lnx2)	5′ flanking, first exon, part of first intron
AC, AG	7 (30230441–697)	Gene model 1082 (Gm1082)	Completely within exon 12
TA, AT	7 (45975389–956)	ATP-binding cassette, sub-family C (CFTR/MRP), member 8 (Abcc8)	Completely within intron 33
TT, AT	17 (4581782–2093)	U6 snRNA	52.409 kb upstream from transcription start site
TT, TT	17 (23405050–489)	Tumor necrosis factor receptor superfamily, member 12a (Tnfrsf12a)	5′ flanking and part of first exon
AT, AA	17 (23882051–423)	Amidohydrolase domain containing 2 (Amdhd2)	1.032 kb downstream from 3′ end of exon 11

[a]Primer pair indicates which 2 of the 8 possible oligos were used to amplify the digested, ligated ChIP DNA (see Materials and Methods).
[b]Absolute position refers to the chromosomal location of *Ava*II-digestible fragments that were picked up by the CD screen. Annotation is based on the NCBI m36 mouse assembly.

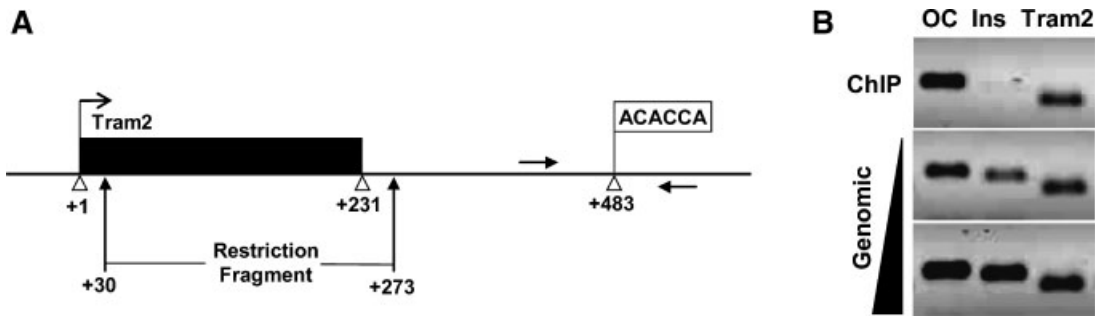

Fig. 2. Runx2 interacts with *Tram2*. **A**: A restriction fragment from the CD screen (*bounded by vertical arrows*) is shown in its genomic context, where it overlaps the first exon of Tram2 (*black rectangle*). Positions are numbered relative to the Tram2 transcription start site (+1). Primers used for conventional ChIP assay (*horizontal arrows*) flank a perfect Runx2 consensus motif (*ACACCA*). **B**: Conventional Runx2 ChIP assay was performed with locus-specific primers flanking the Tram2 Runx2 motif shown in **Panel A**. The region containing the Runx2 element from the murine osteocalcin (*OC*) promoter [Ducy and Karsenty, 1995; Banerjee et al., 1997] was amplified as a positive control, and a region from the insulin promoter (*Ins*) served as negative control. The sequences of the primers used to amplify the *Tram2, OC* and *Ins* regions are provided in Table I. Increasing amounts of *genomic* DNA were also amplified with the same primers under the same conditions, to show that the PCR was performed within a dynamic range. All PCR products were visualized on a 1% agarose gel stained with ethidium bromide.

mouse primary skeletal myoblasts retrovirally infected with Runx2. As shown in Figure 3A, these cells expressed osteocalcin, a classical Runx2 target gene at levels 100-fold higher than unmodified myoblasts. Surprisingly, Tram2 mRNA was 4.5-fold lower in the Runx2-infected cells. These results suggest that Runx2 inhibits, rather than stimulates expression of Tram2. The ability of Runx2 to stimulate and repress different genes, even in the same cells, has been previously described [Javed et al., 2001] and is attributable to the presence of both activation and repression domains in Runx2 [Westendorf, 2006].

We further investigated the influence of Runx2 on Tram2 in C3H10T1/2 mouse embryonic fibroblasts transiently transfected with Runx2. As shown in Figure 3B, Tram2 mRNA levels in Runx2-transfected cells were approximately half of those observed in control cells. Thus, Tram2 expression was inhibited in two different cell lines both after prolonged expression of Runx2 (Fig. 3A) and 48 h following transient transfection of Runx2 (Fig. 3B).

Tram2 is Positively Regulated Along With Osteocalcin Late During BMP-2-Induced Osteoblastic Differentiation of C3H10T1/2 Mouse Embryonic Fibroblasts

BMP signaling plays a major role in osteoblast differentiation, and also modifies Runx2 activity [Lee et al., 2000; Xiao et al., 2002; Guicheux et al., 2003; Chen et al., 2004; Jeon et al., 2006]. We therefore measured Tram2 mRNA levels in C3H10T1/2 cells that were both transfected with Runx2 and treated with BMP-2 recombinant human bone morphogenetic protein 2 (BMP-2). As shown in Figure 3C, the inhibitory effect of Runx2 on Tram2 gene expression was almost completely alleviated in the presence of BMP-2. Thus, the Runx2-mediated inhibition of Tram2 expression was strongest in primary skeletal myoblasts, weaker in naive untreated pluripotent C3H10T1/2 cells, and nearly absent in BMP-2-treated C3H10T1/2 cells.

Given the ability of BMP-2 to modify the effect of exogenous Runx2 on Tram2 expression in transiently transfected C3H10T1/2 cells, we next investigated whether there was any evidence that endogenous Runx2 contributes to the regulation of Tram2 expression in long-term C3H10T1/2 cultures, treated or untreated with BMP-2. As shown in Figure 4A, Runx2 mRNA was detectable in confluent cultures (day 0), and was thereafter up-regulated in both untreated and BMP-2-treated cells. After 2 days of treatment, Runx2 mRNA continued to increase in the BMP-2-treated but not in the untreated cells. Interestingly, expression of OC, a classical Runx2 target gene, was hardly detectable in either untreated or BMP-2-treated cultures on day 4, when Runx2 expression was maximal. Only later did OC mRNA increase and this was only observed in the BMP-2-treated cultures (Fig. 4B). Tram2 expression in untreated cultures increased between day 0 and 1, in parallel to the increase in Runx2 expression. Later, when BMP-2 stimulated Runx2 expression, Tram2 responded similar to OC. Specifically, it

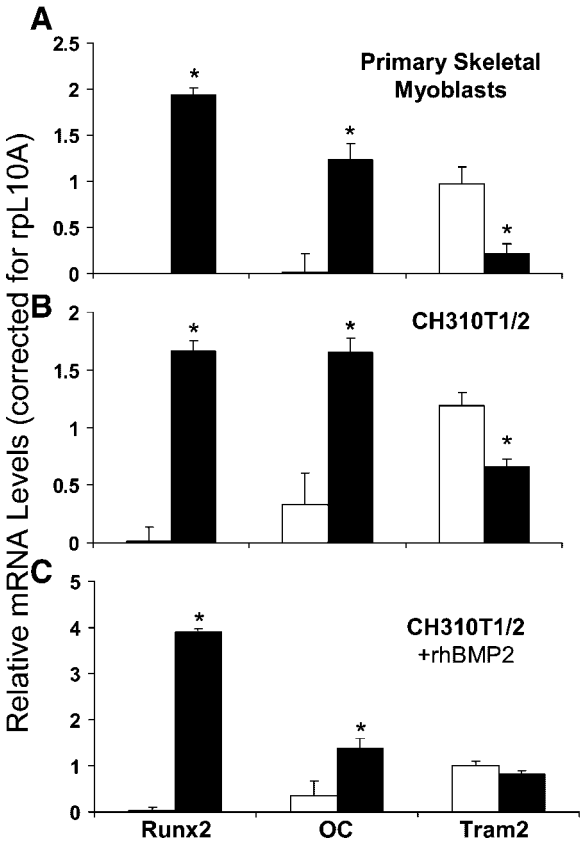

Fig. 3. Runx2 inhibits Tram2 expression in non-osteoblasts. **A**: Primary skeletal myoblasts retrovirally transduced with Runx2 (*black bars*) and unmodified myoblasts (*white bars*) were cultured for 7 days, after which total RNA was extracted and converted to cDNA. *Runx2*, *Osteocalcin* (*OC*), and *Tram2* expression levels were then determined by qPCR. Bars represent the Mean ± SEM (n = 3) of values corrected for the expression of ribosomal protein L10A, whose mRNA levels were not affected by Runx2 overexpression. **B**: C3H10T1/2 mouse embryonic fibroblasts were cultured for 48 h after transient transfection with Runx2 expression construct (*black bars*) or empty vector (*white bars*). Total RNA was collected, reverse-transcribed, and analyzed as described for **Panel A**. Transfection efficiency was approximately 80%, as indicated by FACS analysis of parallel cultures transfected with pGFP-C1 (Clontech). **C**: Same as in **Panel B**, except 300 ng/ml rhBMP-2 was administered for 24 h prior to harvest; $^*P \leq 0.05$.

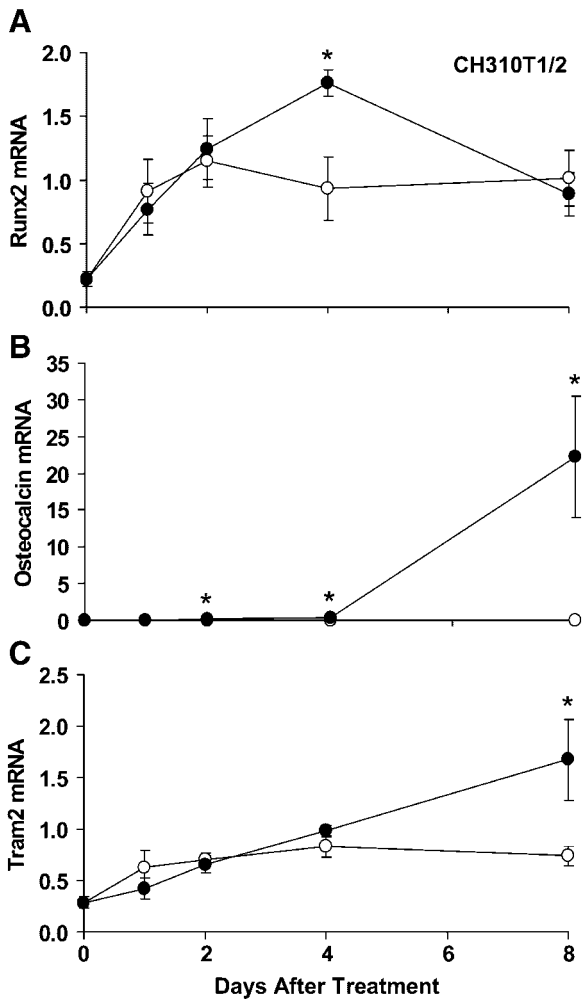

Fig. 4. Upregulation of Tram2 mRNA in BMP-2-treated embryonic fibroblasts. CH310T1/2 cells were cultured in the presence (*closed circles*) or absence (*open circles*) of 300 ng/ml rhBMP-2, and total RNA was collected at the indicated times. Relative mRNA levels were determined by RT-qPCR for (**A**) *Runx2*, (**B**) *Osteocalcin* (*OC*), and (**C**) *Tram2*. All data points are the Means ± SEM (n = 3) of values corrected for the expression of ribosomal protein L10A, whose mRNA was not affected by BMP-2 treatment; $^*P \leq 0.05$.

was not influenced by BMP-2 until day 4, even though by this point Runx2 mRNA levels had already peaked. Thereafter, however, Tram2 expression was higher in the presence of BMP-2 (day 8), like that of OC mRNA. The similarity between Tram2 and OC expression observed after Runx2 is induced by BMP-2 treatment suggests that Runx2 positively regulates Tram2 transcription during the latter stages of osteogenic differentiation in the C3H10T1/2 culture model.

Tram2 is Up-Regulated Soon after BMP-2 Treatment of ST2 Bone Marrow-Derived Stromal Cell

We further investigated Tram2 expression during BMP-2-mediated osteogenic differentiation of ST2 bone marrow-derived stromal cell cultures. As shown in Figure 5A, Runx2 mRNA was detectable in confluent ST2 cultures (day 0), and was thereafter increased in both untreated and BMP-2-treated cells. However, after 2 days of treatment, Runx2 mRNA was expressed at higher levels in the cells treated

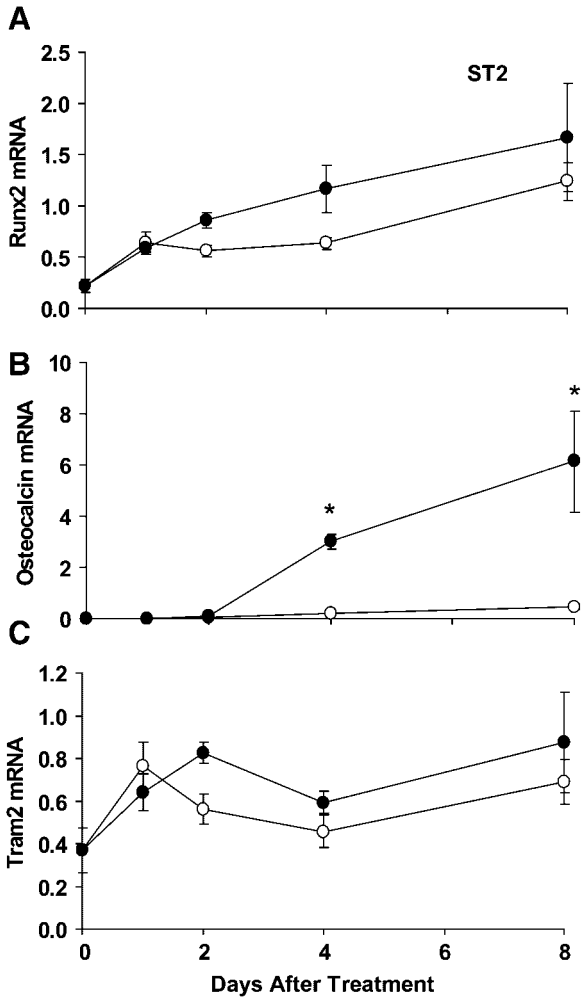

Fig. 5. Early upregulation of Tram2 mRNA in rhBMP-2 treated bone marrow-derived stromal cells. ST2 cells were cultured and treated following the same protocol as in Figure 4. Gene expression was analyzed and the data was plotted as in Figure 4 for (**A**) *Runx2*, (**B**) *Osteocalcin* (*OC*), and (**C**) *Tram2*. *Closed circles*, rhBMP-2 (300 ng/ml); *open circles*, control. Mean ± SEM (n = 3); $^*P \leq 0.05$.

with BMP-2. At this time point, OC mRNA was still hardly detectable. OC expression commenced after day 2, and was remarkably stronger in the BMP-2-treated cultures (Fig. 5B). Interestingly, Tram2 mRNA, which, unlike OC, was already detected on day 0, responded to BMP-2 treatment as early as day 2, at which Runx2 was first upregulated in the treated compared to untreated cultures (Fig. 5C). These results are consistent with Runx2 controlling Tram2 gene expression; the earlier response of Tram2 compared to OC likely reflects the inactivity of positive regulatory mechanisms, or the activity of negative regulatory mechanisms, which result in lack of basal OC expression on day 2.

Runx2, Osteocalcin and Tram2 are Transiently Upregulated in BMP-2-Treated C2C12 Myoblasts

C2C12 myoblasts undergo transdifferentiation and acquire an osteoblast-like phenotype in response to BMP-2 treatment [Katagiri et al., 1994]. This transdifferentiation entails the induction and activation of Runx2 and Runx2 target genes [Lee et al., 2000]. We observed transient upregulation of Runx2 in post-confluent C2C12 cultures even in the absence of BMP-2 (Fig. 6A); however, this upregulation was brief, and was not

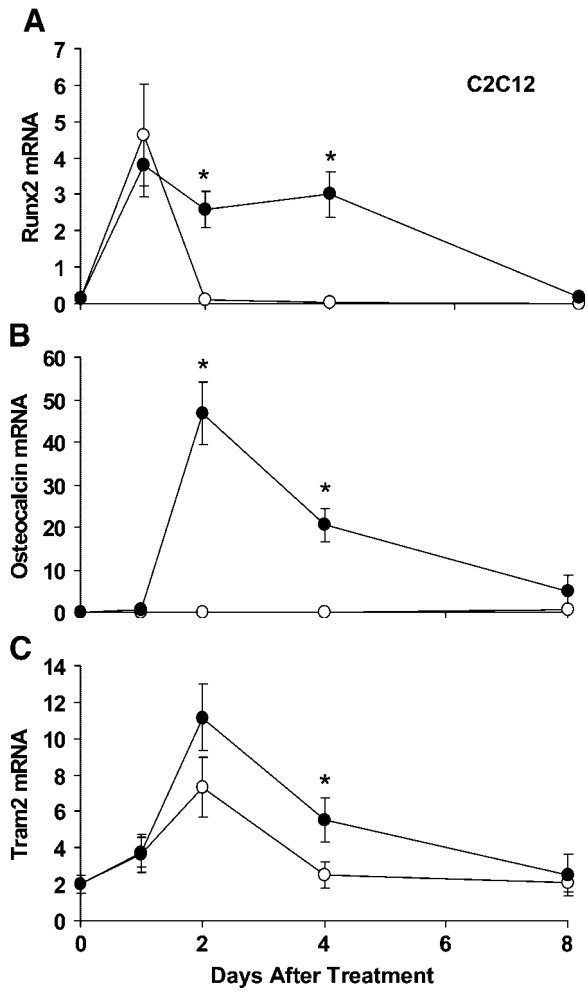

Fig. 6. Transient upregulation of Tram2 mRNA in BMP-2 treated C2C12 pre-myoblasts. Gene expression in C2C12 cell cultures was measured under the same conditions described in Figures 4 and 5. Each data point is the Mean expression ± SEM (n = 3) of (**A**) *Runx2*, (**B**) *Osteocalcin* (*OC*), and (**C**) *Tram2*. *Closed circles*, BMP-2 (300 ng/ml); *open circles*, control. $^*P \leq 0.05$.

accompanied by an induction of OC mRNA (Fig. 6B). In contrast, the upregulation of Runx2 mRNA in BMP-2-treated cells was sustained for several days, and was followed by similar upregulation of OC mRNA. The Tram2 expression profile in the BMP-2-treated cultures paralleled that of OC, with both mRNAs reaching maximum levels on day 2 (Fig. 6B,C). However, reminiscent of the ST2 cells, the C2C12 cultures already expressed Tram2, but not OC, on day 0 (Fig. 6B,C). By day 2, Tram2 mRNA in untreated cultures was slightly upregulated in parallel to the brief expression of Runx2. As compared to the untreated cultures, the BMP-2-treated cultures had 1.5-fold more Tram2 mRNA on day 2, and 2.2-fold more Tram2 mRNA on day 4, as basal levels declined (Fig. 6C).

Tram2 Expression in MC3T3-E1 Osteoblastic Cells is Regulated by BMP-2 in a Developmental Stage-Specific Manner

We finally investigated the expression pattern of Tram2 in MC3T3-E1 preosteoblasts, in which the physical interaction of this gene with Runx2 was originally discovered (Figs. 1 and 2). In BMP-2-treated cultures, Tram2 mRNA levels behave like those of OC after Runx2 activation. That is, they steadily increase from day 1 throughout the remainder of the time course (Fig. 7B,C). Interestingly, Tram2 expression does not parallel that of Runx2 in the absence of BMP-2. Between day 0 and 1, there is a dramatic increase in Tram2 mRNA with an antiparallel decrease in Runx2 mRNA; thereafter, Tram2 mRNA levels decrease as Runx2 levels increase (Fig. 7A,C). The inverse relationship between Runx2 and Tram2 in untreated MC3T3-E1 cells is reminiscent of the results with primary myoblasts (Fig. 3A) and untreated C3H10T1/2 cells (Fig. 3B). In the same untreated MC3T3-E1 cells, OC mRNA is undetectable until day 2 (Fig. 7B). Thereafter, it increases in parallel to Runx2 mRNA (Fig. 7A,B), suggesting differential regulation of OC versus Tram2 transcription by Runx2 in untreated MC3T3-E1 cells.

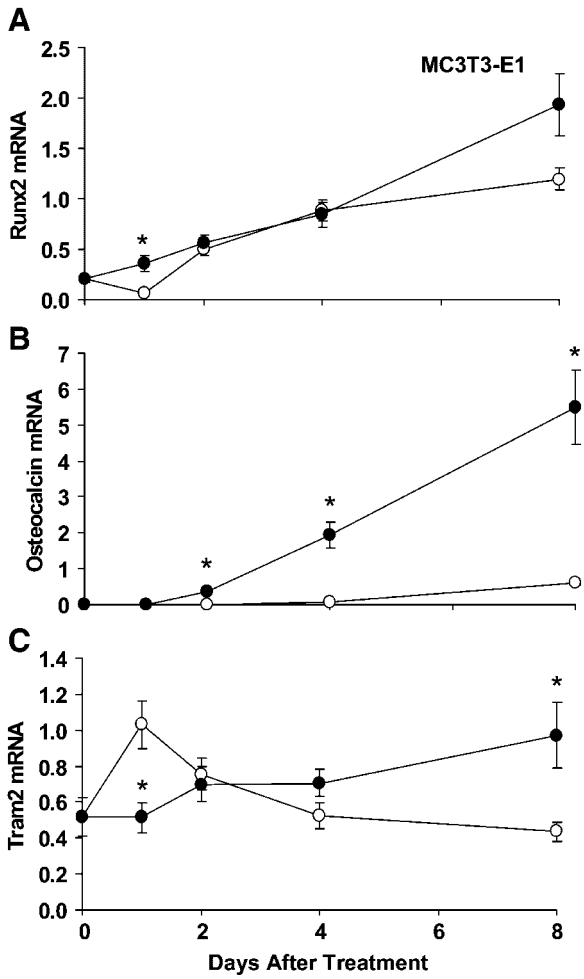

Fig. 7. Tram2 expression in osteoblastic cells is regulated by BMP-2 in a developmental stage-specific manner. MC3T3-E1 cells were cultured in the presence (*closed circles*) or absence (*open circles*) of 300 ng/ml rhBMP-2, and total RNA was collected at the indicated times. Relative mRNA levels were determined by RT-qPCR for (**A**) *Runx2*, (**B**) *Osteocalcin* (*OC*), and (**C**) *Tram2*. Each data point represents the Mean ± SEM (n = 3) of values corrected for the expression of ribosomal protein L10A, whose mRNA was not affected by BMP-2 treatment. $^*P \leq 0.05$.

DISCUSSION

Using CD of MC3T3-E1 osteoblasts, we discovered seven Runx2 genomic sites that were not previously known to be occupied by Runx2 in living cells. Unlike location analyses of other transcription factors, where many occupied sites were found tens of kb away from nearby known genes, our results suggest that Runx2 may occupy regions that tend to be associated with transcribed sequences. All but one of the 12 Runx2 occupied regions in our present and previous study were either within annotated genes or up to 1-kb from either end (Table II and Barski and Frenkel [2004]). Of the 11 intragenic Runx2 sites, 6 were either within or overlapping the first intron. Albeit limited in scope, these results also highlight the evolving concept that *cis*-acting regulatory elements are not

necessarily confined to 5′ flanking gene sequences [Cawley et al., 2004; Bieda et al., 2006], but suggest that Runx2-occupied regions are frequently found within or 3′ to transcribed sequences. One of our Runx2 hits was in the first intron of Tram2, immediately downstream of the first, 231-bp long exon. The evidence that Tram2 is regulated by Runx2 include: (1) Tram2 mRNA is downregulated in response to ectopic Runx2 expression in primary skeletal myoblasts and C3H10T1/2 embryonic fibroblasts; and (2) Tram2 expression parallels that of osteocalcin in the BMP-2-treated C3H10T1/2, ST2, C2C12, and MC3T3-E1 cell lines. The apparently opposing effects of Runx2 on Tram2 expression in the different experimental systems may represent alterations in Runx2 activity at the Tram2 locus as a function of cell type or developmental stage (see below). Be that as it may, given the role of Tram2 in type I collagen synthesis [Stefanovic et al., 2004], and given the role of type I collagen in bone, it is likely that Tram2 belongs to the machinery engaged by Runx2 in promoting osteoblast differentiation and function.

Cell Type-Dependent and Gene-Specific Transcriptional Regulation by Runx2

Runx2 has been shown to function as a transcriptional activator or repressor depending on the cellular milieu and promoter context [Javed et al., 2001]. We provide further evidence of this by showing that Runx2 is associated with either Tram2 repression or activation depending on the cell type and culture conditions. Further, in some instances, for example, primary myoblasts, Runx2 repressed Tram2 while activating osteocalcin expression. These phenomena are likely explained by the involvement of co-regulators that either stimulate or repress Runx2 transcriptional activity. Transcription factors that positively modify Runx2's activity include Cbfβ [Yoshida et al., 2002], C/EBPβ and C/EBPδ [Gutierrez et al., 2002], ETS1 [Sato et al., 1998a], Menin [Sowa et al., 2004], Smad1 [Zhang et al., 2000], Smad5 [Nishimura et al., 2002], Grg5 [Wang et al., 2004], Rb [Thomas et al., 2001], TAZ [Cui et al., 2003], and p204 [Liu et al., 2005], whereas negative co-regulators of Runx2's activity include C/EBPδ [McCarthy et al., 2000], Dlx3 [Hassan et al., 2004], Msx2 [Shirakabe et al., 2001], PPARγ [Jeon et al., 2003], HDAC4 [Vega et al., 2004], HDAC3 [Schroeder et al., 2004], Stat1 [Kim et al., 2003], Twist [Bialek et al., 2004], Yes [Zaidi et al., 2004], TLE [Javed et al., 2000], and Smad3 [Kang et al., 2005]. Thus, the ability of Runx2 to exert different effects on the same gene in different cells may be due to the differential expression of co-regulators among cell types. Likewise, the ability of Runx2 to exert opposing effects on different genes in the same cell may be due to preferential recruitment of coactivators or corepressors, depending on the sequences in the vicinity of the Runx2 binding site. Finally, it is conceivable that particular genes may be initially stimulated and then repressed by Runx2 during development of the osteoblast phenotype. The biphasic expression pattern of Tram2 as a function of time in MC3T3-E1 and C2C12 cultures may reflect such transition in Runx2 activity at this locus.

BMP-Dependent Transcriptional Regulation by Runx2

BMPs are potent osteogenic agents [Chen et al., 2004], in part due to their ability to upregulate Runx2 expression [Lee et al., 1999]. While BMP-2 treatment does not increase the interaction of Runx2 with the OC promoter in MC3T3-E1 cells (our unpublished ChIP results), several mechanisms have been reported, through which BMPs post-translationally enhance Runx2 transcriptional activity. For example, p300-mediated acetylation of Runx2 is induced by BMP-2, and this prevents Smurf-mediated degradation of Runx2 [Jeon et al., 2006]. Also, Runx2 is a substrate for MAPK [Xiao et al., 2002], which in turn can be activated by BMP signaling [Guicheux et al., 2003]. Finally, Smad-1, -5, and -8, which are activated by BMPs, can associate with and augment Runx2-mediated transcription [Lee et al., 2000]. Consistent with these notions, we show here that (i) the Runx2-mediated repression of Tram2 in C3H10T1/2 cells was alleviated by the addition of BMP-2, (ii) BMP-2 enhanced Runx2 and Tram2 levels compared to untreated cells in the four cell lines tested; and (iii) the relationship between Tram2 and Runx2 expression in MC3T3-E1 cells was completely reversed upon treatment with BMP-2. A likely interpretation of these results is that BMP-2 altered the Runx2-mediated regulation of Tram2. However, we cannot rule out BMP-dependent Runx2-indepedent regulation of Tram2 expression.

Potential Novel Mediators of Osteoblast Development and Function

The present study identifies translocon-associated membrane protein 2 (Tram2) as a Runx2 target gene. Tram2 was originally identified in a microarray screen for genes stimulated in a stellate cell culture model of cirrhosis [Stefanovic et al., 2004]. Most of the Tram2 domains are highly homologous to TRAM, an integral component of the protein translocon found on the endoplasmic reticulum (ER). The C-terminus of Tram2, which shares only 15% homology with Tram, was found to interact with Serca2b, the Ca^{2+} pump of the ER [Stefanovic et al., 2004], and over-expression of a Tram2 deletion mutant lacking the C-terminus resulted in decreased collagen accumulation. Since depletion of ER Ca^{2+} stores had a similar effect, the authors proposed that Tram2 may recruit Serca2b to the translocon, leading to increased local Ca^{2+} concentration and stimulation of chaperone-mediated folding of triple helical procollagen [Stefanovic et al., 2004]. Like activated stellate cells, osteoblasts produce large amounts of type I collagen. Runx2 may promote osteoblast differentiation and function by enhancing the transcription of not only type I collagen [Kern et al., 2001], but also genes like Tram2, which are necessary for effective post-translational processing of this macromolecule.

Other Runx2 target genes identified in this study may also help explain the importance of Runx2 in skeletogenesis. Numb is an inhibitor of Notch signaling in Drosophila [Guo et al., 1996; Spana and Doe, 1996], and likely in mammalian cells as well [Petersen et al., 2006], and Notch signaling plays an important role in osteoblast differentiation [Deregowski et al., 2006]. We have found that Runx2 occupies the gene encoding Ligand of Numb-related protein 2 (Lnx2), a scaffolding molecule for mammalian Numb and Numblike [Rice et al., 2001]. It is conceivable that regulation of Lnx2 by Runx2 contributes to the osteogenic program.

Another gene that was associated with Runx2 in living MC3T3-E1 osteoblastic cells is Tumor necrosis factor receptor super-family 12a (TNFRsf12a). Stimulation of this TNF-like receptor in MC3T3-E1 cells results in concomitant inhibition of osteoblast differentiation and induction of the osteoclast activators RANKL and RANTES [Ando et al., 2006]. Regulation of TNFRsf12a by Runx2 might therefore play a role in modulating the activities of both osteoblasts and osteoclasts.

In summary, we used CD to identify seven genomic loci that are occupied by Runx2 in developing MC3T3-E1 pre-osteoblasts. Expression of one of these genes, Tram2, is regulated by Runx2 in a manner dependent upon cell type and the status of the BMP signaling pathway. Further investigation is warranted to delineate the potential roles of Tram2 and the other novel Runx2 targets in bone biology, as well as to expand the repertoire of Runx2-regulated genes in osteoblasts.

ACKNOWLEDGMENTS

We thank Dr. Gerard Karsenty for the Runx2 expression vector and Wyeth Pharmaceuticals (Cambridge MA) for rhBMP-2. This study was supported by grant DK071122 (to BF) and EB003364 (to AJG) from the NIH and by the J. Harold and Edna L. LaBriola Chair in Genetic Orthopaedics at the University of Southern California (held by BF). SP was partially supported by NIH training grant T 32 GM067587. The experiments were conducted in a facility constructed with support from Research Facilities Improvement Program Grant Number C06 (RR10600-01, CA62528-01, RR14514-01) from the NIH/NCRR.

REFERENCES

Ando T, Ichikawa J, Wako M, Hatsushika K, Watanabe Y, Sakuma M, Tasaka K, Ogawa H, Hamada Y, Yagita H, Nakao A. 2006. TWEAK/Fn14 interaction regulates RANTES production, BMP-2-induced differentiation, and RANKL expression in mouse osteoblastic MC3T3-E1 cells. Arthritis Res Ther 8:R146.

Aubin JE, Gupta AK, Zirngbl R, Rossant J. 1996. Knockout mice lacking bone sialoprotein expression have bone abnormalities. J Bone Miner Res 11 (supplement 1):S102. (abstract).

Banerjee C, McCabe LR, Choi JY, Hiebert SW, Stein JL, Stein GS, Lian JB. 1997. Runt homology domain proteins in osteoblast differentiation: AML3/CBFA1 is a major component of a bone-specific complex. J Cell Biochem 66:1–8.

Barski A, Frenkel B. 2004. ChIP display: Novel method for identification of genomic targets of transcription factors. Nucleic Acids Res 32:e104.

Bialek P, Kern B, Yang X, Schrock M, Sosic D, Hong N, Wu H, Yu K, Ornitz DM, Olson EN, Justice MJ, Karsenty G. 2004. A twist code determines the onset of osteoblast differentiation. Dev Cell 6:423–435.

Bieda M, Xu X, Singer MA, Green R, Farnham PJ. 2006. Unbiased location analysis of E2F1-binding sites

suggests a widespread role for E2F1 in the human genome. Genome Res 16:595–605.

Bryan J, Munoz A, Zhang X, Dufer M, Drews G, Krippeit-Drews P, Aguilar-Bryan L. 2007. ABCC8 and ABC C9: ABC transporters that regulate K(+) channels. Pflugers Arch 453:703–718.

Bucay N, Sarosi I, Dunstan CR, Morony S, Tarpley J, Capparelli C, Scully S, Tan HL, Xu W, Lacey DL, Boyle WJ, Simonet WS. 1998. osteoprotegerin-deficient mice develop early onset osteoporosis and arterial calcification. Genes Dev 12:1260–1268.

Cawley S, Bekiranov S, Ng HH, Kapranov P, Sekinger EA, Kampa D, Piccolboni A, Sementchenko V, Cheng J, Williams AJ, Wheeler R, Wong B, Drenkow J, Yamanaka M, Patel S, Brubaker S, Tammana H, Helt G, Struhl K, Gingeras TR. 2004. Unbiased mapping of transcription factor binding sites along human chromosomes 21 and 22 points to widespread regulation of noncoding RNAs. Cell 116:499–509.

Chen J, Sadowski I. 2005. Identification of the mismatch repair genes PMS2 and MLH1 as p53 target genes by using serial analysis of binding elements. Proc Natl Acad Sci USA 102:4813–4818.

Chen D, Zhao M, Mundy GR. 2004. Bone morphogenetic proteins. Growth Factors 22:233–241.

Colnot C, Fowlis D, Ripoche MA, Bouchaert I, Poirier F. 1998. Embryonic implantation in galectin 1/galectin 3 double mutant mice. Dev Dyn 211:306–313.

Cui CB, Cooper LF, Yang X, Karsenty G, Aukhil I. 2003. Transcriptional coactivation of bone-specific transcription factor Cbfa1 by TAZ. Mol Cell Biol 23:1004–1013.

Deregowski V, Gazzerro E, Priest L, Rydziel S, Canalis E. 2006. Notch 1 overexpression inhibits osteoblastogenesis by suppressing Wnt/beta-catenin but not bone morphogenetic protein signaling. J Biol Chem 281:6203–6210.

Doecke JD, Day CJ, Stephens AS, Carter SL, van Daal A, Kotowicz MA, Nicholson GC, Morrison NA. 2006. Association of functionally different RUNX2 P2 promoter alleles with BMD. J Bone Miner Res 21:265–273.

Ducy P, Karsenty G. 1995. Two distinct osteoblast-specific cis-acting elements control expression of a mouse osteocalcin gene. Mol Cell Biol 15:1858–1869.

Ducy P, Desbois C, Boyce B, Pinero G, Story B, Dunstan C, Smith E, Bonadio J, Goldstein S, Gundberg C, Bradley A, Karsenty G. 1996. Increased bone formation in osteocalcin-deficient mice. Nature 382:448–452.

Ducy P, Zhang R, Geoffroy V, Ridall AL, Karsenty G. 1997. Osf2/Cbfa1: A transcriptional activator of osteoblast differentiation. Cell 89:747–754.

Ducy P, Starbuck M, Priemel M, Shen J, Pinero G, Geoffroy V, Amling M, Karsenty G. 1999. A Cbfa1-dependent genetic pathway controls bone formation beyond embryonic development. Genes Dev 13:1025–1036.

Geoffroy V, Kneissel M, Fournier B, Boyde A, Matthias P. 2002. High bone resorption in adult aging transgenic mice overexpressing cbfa1/runx2 in cells of the osteoblastic lineage. Mol Cell Biol 22:6222–6233.

Gersbach CA, Le Doux JM, Guldberg RE, Garcia AJ. 2006. Inducible regulation of Runx2-stimulated osteogenesis. Gene Ther 13:873–882.

Guicheux J, Lemonnier J, Ghayor C, Suzuki A, Palmer G, Caverzasio J. 2003. Activation of p38 mitogen-activated protein kinase and c-Jun-NH2-terminal kinase by BMP-2 and their implication in the stimulation of osteoblastic cell differentiation. J Bone Miner Res 18: 2060–2068.

Guo M, Jan LY, Jan YN. 1996. Control of daughter cell fates during asymmetric division: Interaction of Numb and Notch. Neuron 17:27–41.

Gutierrez S, Javed A, Tennant DK, van Rees M, Montecino M, Stein GS, Stein JL, Lian JB. 2002. CCAAT/enhancer-binding proteins (C/EBP) beta and delta activate osteocalcin gene transcription and synergize with Runx2 at the C/EBP element to regulate bone-specific expression. J Biol Chem 277:1316–1323.

Harada H, Tagashira S, Fujiwara M, Ogawa S, Katsumata T, Yamaguchi A, Komori T, Nakatsuka M. 1999. Cbfa1 isoforms exert functional differences in osteoblast differentiation. J Biol Chem 274:6972–6978.

Hassan MQ, Javed A, Morasso MI, Karlin J, Montecino M, van Wijnen AJ, Stein GS, Stein JL, Lian JB. 2004. Dlx3 transcriptional regulation of osteoblast differentiation: Temporal recruitment of Msx2, Dlx3, and Dlx5 homeodomain proteins to chromatin of the osteocalcin gene. Mol Cell Biol 24:9248–9261.

Hecht J, Seitz V, Urban M, Wagner F, Robinson PN, Stiege A, Dieterich C, Kornak U, Wilkening U, Brieske N, Zwingman C, Kidess A, Stricker S, Mundlos S. 2007. Detection of novel skeletogenesis target genes by comprehensive analysis of a Runx2(−/−) mouse model. Gene Expr Patterns 7:102–112.

Horak CE, Snyder M. 2002. ChIP-chip: A genomic approach for identifying transcription factor binding sites. Methods Enzymol 350:469–483.

Impey S, McCorkle SR, Cha-Molstad H, Dwyer JM, Yochum GS, Boss JM, McWeeney S, Dunn JJ, Mandel G, Goodman RH. 2004. Defining the CREB regulon: A genome-wide analysis of transcription factor regulatory regions. Cell 119:1041–1054.

Inada M, Wang Y, Byrne MH, Rahman MU, Miyaura C, Lopez-Otin C, Krane SM. 2004. Critical roles for collagenase-3 (Mmp13) in development of growth plate cartilage and in endochondral ossification. Proc Natl Acad Sci USA 101:17192–17197.

Irizarry RA, Warren D, Spencer F, Kim IF, Biswal S, Frank BC, Gabrielson E, Garcia JG, Geoghegan J, Germino G, Griffin C, Hilmer SC, Hoffman E, Jedlicka AE, Kawasaki E, Martinez-Murillo F, Morsberger L, Lee H, Petersen D, Quackenbush J, Scott A, Wilson M, Yang Y, Ye SQ, Yu W. 2005. Multiple-laboratory comparison of microarray platforms. Nat Methods 2:345–350.

Javed A, Guo B, Hiebert S, Choi JY, Green J, Zhao SC, Osborne MA, Stifani S, Stein JL, Lian JB, van Wijnen AJ, Stein GS. 2000. Groucho/TLE/R-esp proteins associate with the nuclear matrix and repress RUNX (CBF(alpha)/AML/PEBP2(alpha)) dependent activation of tissue-specific gene transcription. J Cell Sci 113(Pt 12):2221–2231.

Javed A, Barnes GL, Jasanya BO, Stein JL, Gerstenfeld L, Lian JB, Stein GS. 2001. Runt homology domain transcription factors (Runx, Cbfa, and AML) mediate repression of the bone sialoprotein promoter: Evidence for promoter context-dependent activity of Cbfa proteins. Mol Cell Biol 21:2891–2905.

Jeon MJ, Kim JA, Kwon SH, Kim SW, Park KS, Park SW, Kim SY, Shin CS. 2003. Activation of peroxisome proliferator-activated receptor-gamma inhibits the

Runx2-mediated transcription of osteocalcin in osteoblasts. J Biol Chem 278:23270–23277.

Jeon EJ, Lee KY, Choi NS, Lee MH, Kim HN, Jin YH, Ryoo HM, Choi JY, Yoshida M, Nishino N, Oh BC, Lee KS, Lee YH, Bae SC. 2006. Bone morphogenetic protein-2 stimulates Runx2 acetylation. J Biol Chem 281:16502–16511.

Jimenez MJ, Balbin M, Lopez JM, Alvarez J, Komori T, Lopez-Otin C. 1999. Collagenase 3 is a target of Cbfa1, a transcription factor of the runt gene family involved in bone formation. Mol Cell Biol 19:4431–4442.

Kang JS, Alliston T, Delston R, Derynck R. 2005. Repression of Runx2 function by TGF-beta through recruitment of class II histone deacetylases by Smad3. EMBO J 24:2543–2555.

Katagiri T, Yamaguchi A, Komaki M, Abe E, Takahashi N, Ikeda T, Rosen V, Wozney JM, Fujisawa-Sehara A, Suda T. 1994. Bone morphogenetic protein-2 converts the differentiation pathway of C2C12 myoblasts into the osteoblast lineage. J Cell Biol 127:1755–1766.

Kern B, Shen J, Starbuck M, Karsenty G. 2001. Cbfa1 contributes to the osteoblast-specific expression of type I collagen genes. J Biol Chem 276:7101–7107.

Kim S, Koga T, Isobe M, Kern BE, Yokochi T, Chin YE, Karsenty G, Taniguchi T, Takayanagi H. 2003. Stat1 functions as a cytoplasmic attenuator of Runx2 in the transcriptional program of osteoblast differentiation. Genes Dev 17:1979–1991.

Kim J, Bhinge AA, Morgan XC, Iyer VR. 2005. Mapping DNA-protein interactions in large genomes by sequence tag analysis of genomic enrichment. Nat Methods 2:47–53.

Komori T, Yagi H, Nomura S, Yamaguchi A, Sasaki K, Deguchi K, Shimizu Y, Bronson RT, Gao YH, Inada M, Sato M, Okamoto R, Kitamura Y, Yoshiki S, Kishimoto T. 1997. Targeted disruption of Cbfa1 results in a complete lack of bone formation owing to maturational arrest of osteoblasts. Cell 89:755–764.

Lee MH, Javed A, Kim HJ, Shin HI, Gutierrez S, Choi JY, Rosen V, Stein JL, van Wijnen AJ, Stein GS, Lian JB, Ryoo HM. 1999. Transient upregulation of CBFA1 in response to bone morphogenetic protein-2 and transforming growth factor beta1 in C2C12 myogenic cells coincides with suppression of the myogenic phenotype but is not sufficient for osteoblast differentiation. J Cell Biochem 73:114–125.

Lee KS, Kim HJ, Li QL, Chi XZ, Ueta C, Komori T, Wozney JM, Kim EG, Choi JY, Ryoo HM, Bae SC. 2000. Runx2 is a common target of transforming growth factor beta1 and bone morphogenetic protein 2, and cooperation between Runx2 and Smad5 induces osteoblast-specific gene expression in the pluripotent mesenchymal precursor cell line C2 C12. Mol Cell Biol 20:8783–8792.

Liu W, Toyosawa S, Furuichi T, Kanatani N, Yoshida C, Liu Y, Himeno M, Narai S, Yamaguchi A, Komori T. 2001. Overexpression of Cbfa1 in osteoblasts inhibits osteoblast maturation and causes osteopenia with multiple fractures. J Cell Biol 155:157–166.

Liu CJ, Chang E, Yu J, Carlson CS, Prazak L, Yu XP, Ding B, Lengyel P, Di Cesare PE. 2005. The interferon-inducible p204 protein acts as a transcriptional coactivator of Cbfa1 and enhances osteoblast differentiation. J Biol Chem 280:2788–2796.

Loh YH, Wu Q, Chew JL, Vega VB, Zhang W, Chen X, Bourque G, George J, Leong B, Liu J, Wong KY, Sung KW, Lee CW, Zhao XD, Chiu KP, Lipovich L, Kuznetsov VA, Robson P, Stanton LW, Wei CL, Ruan Y, Lim B, Ng HH. 2006. The Oct4 and Nanog transcription network regulates pluripotency in mouse embryonic stem cells. Nat Genet 38:431–440.

McCarthy TL, Ji C, Chen Y, Kim KK, Imagawa M, Ito Y, Centrella M. 2000. Runt domain factor (Runx)-dependent effects on CCAAT/ enhancer-binding protein delta expression and activity in osteoblasts. J Biol Chem 275: 21746–21753.

Meyers S, Downing JR, Hiebert SW. 1993. Identification of AML-1 and the (8;21) translocation protein (AML-1/ETO) as sequence-specific DNA-binding proteins: the runt homology domain is required for DNA binding and protein-protein interactions. Mol Cell Biol 13:6336–6345.

Mizuno A, Amizuka N, Irie K, Murakami A, Fujise N, Kanno T, Sato Y, Nakagawa N, Yasuda H, Mochizuki S, Gomibuchi T, Yano K, Shima N, Washida N, Tsuda E, Morinaga T, Higashio K, Ozawa H. 1998. Severe osteoporosis in mice lacking osteoclastogenesis inhibitory factor/osteoprotegerin. Biochem Biophys Res Commun 247:610–615.

Mundlos S, Otto F, Mundlos C, Mulliken JB, Aylsworth AS, Albright S, Lindhout D, Cole WG, Henn W, Knoll JH, Owen MJ, Mertelsmann R, Zabel BU, Olsen BR. 1997. Mutations involving the transcription factor CBFA1 cause cleidocranial dysplasia. Cell 89:773–779.

Murshed M, Harmey D, Millan JL, McKee MD, Karsenty G. 2005. Unique coexpression in osteoblasts of broadly expressed genes accounts for the spatial restriction of ECM mineralization to bone. Genes Dev 19:1093–1104.

Nishimura R, Hata K, Harris SE, Ikeda F, Yoneda T. 2002. Core-binding factor alpha 1 (Cbfa1) induces osteoblastic differentiation of C2C12 cells without interactions with Smad1 and Smad5. Bone 31:303–312.

Otto F, Thornell AP, Crompton T, Denzel A, Gilmour KC, Rosewell IR, Stamp GW, Beddington RS, Mundlos S, Olsen BR, Selby PB, Owen MJ. 1997. Cbfa1, a candidate gene for cleidocranial dysplasia syndrome, is essential for osteoblast differentiation and bone development. Cell 89:765–771.

Petersen PH, Tang H, Zou K, Zhong W. 2006. The enigma of the numb-Notch relationship during mammalian embryogenesis. Dev Neurosci 28:156–168.

Prince M, Banerjee C, Javed A, Green J, Lian JB, Stein GS, Bodine PV, Komm BS. 2001. Expression and regulation of Runx2/Cbfa1 and osteoblast phenotypic markers during the growth and differentiation of human osteoblasts. J Cell Biochem 80:424–440.

Ren B, Robert F, Wyrick JJ, Aparicio O, Jennings EG, Simon I, Zeitlinger J, Schreiber J, Hannett N, Kanin E, Volkert TL, Wilson CJ, Bell SP, Young RA. 2000. Genome-wide location and function of DNA binding proteins. Science 290:2306–2309.

Rice DS, Northcutt GM, Kurschner C. 2001. The Lnx family proteins function as molecular scaffolds for Numb family proteins. Mol Cell Neurosci 18:525–540.

Rittling SR, Matsumoto HN, McKee MD, Nanci A, An XR, Novick KE, Kowalski AJ, Noda M, Denhardt DT. 1998. Mice lacking osteopontin show normal development and bone structure but display altered osteoclast formation in vitro. J Bone Miner Res 13:1101–1111.

Roca H, Phimphilai M, Gopalakrishnan R, Xiao G, Franceschi RT. 2005. Cooperative interactions between RUNX2 and homeodomain protein-binding sites are critical for the osteoblast-specific expression of the bone sialoprotein gene. J Biol Chem 280:30845–30855.

Roh TY, Ngau WC, Cui K, Landsman D, Zhao K. 2004. High-resolution genome-wide mapping of histone modifications. Nat Biotechnol 22:1013–1016.

Sato M, Morii E, Komori T, Kawahata H, Sugimoto M, Terai K, Shimizu H, Yasui T, Ogihara H, Yasui N, Ochi T, Kitamura Y, Ito Y, Nomura S. 1998a. Transcriptional regulation of osteopontin gene in vivo by PEBP2alphaA/CBFA1 and ETS1 in the skeletal tissues. Oncogene 17:1517–1525.

Sato M, Yasui N, Nakase T, Kawahata H, Sugimoto M, Hirota S, Kitamura Y, Nomura S, Ochi T. 1998b. Expression of bone matrix proteins mRNA during distraction osteogenesis. J Bone Miner Res 13:1221–1231.

Schroeder TM, Kahler RA, Li X, Westendorf JJ. 2004. Histone deacetylase 3 interacts with runx2 to repress the osteocalcin promoter and regulate osteoblast differentiation. J Biol Chem 279:41998–42007.

Shirakabe K, Terasawa K, Miyama K, Shibuya H, Nishida E. 2001. Regulation of the activity of the transcription factor Runx2 by two homeobox proteins, Msx2 and Dlx5. Genes Cells 6:851–856.

Smith E, Redman RA, Logg CR, Coetzee GA, Kasahara N, Frenkel B. 2000. Glucocorticoids inhibit developmental stage-specific osteoblast cell cycle. Dissociation of cyclin A-cyclin-dependent kinase 2 from E2F4-p130 complexes. J Biol Chem 275:19992–20001.

Sowa H, Kaji H, Hendy GN, Canaff L, Komori T, Sugimoto T, Chihara K. 2004. Menin is required for bone morphogenetic protein 2- and transforming growth factor beta-regulated osteoblastic differentiation through interaction with Smads and Runx2. J Biol Chem 279:40267–40275.

Spana EP, Doe CQ. 1996. Numb antagonizes Notch signaling to specify sibling neuron cell fates. Neuron 17: 21–26.

Stefanovic B, Stefanovic L, Schnabl B, Bataller R, Brenner DA. 2004. TRAM2 protein interacts with endoplasmic reticulum Ca2+ pump Serca2b and is necessary for collagen type I synthesis. Mol Cell Biol 24:1758–1768.

Stickens D, Behonick DJ, Ortega N, Heyer B, Hartenstein B, Yu Y, Fosang AJ, Schorpp-Kistner M, Angel P, Werb Z. 2004. Altered endochondral bone development in matrix metalloproteinase 13-deficient mice. Development 131: 5883–5895.

Stock M, Schafer H, Stricker S, Gross G, Mundlos S, Otto F. 2003. Expression of galectin-3 in skeletal tissues is controlled by Runx2. J Biol Chem 278:17360–17367.

Thirunavukkarasu K, Halladay DL, Miles RR, Yang X, Galvin RJ, Chandrasekhar S, Martin TJ, Onyia JE. 2000. The osteoblast-specific transcription factor Cbfa1 contributes to the expression of osteoprotegerin, a potent inhibitor of osteoclast differentiation and function. J Biol Chem 275:25163–25172.

Thomas DM, Carty SA, Piscopo DM, Lee JS, Wang WF, Forrester WC, Hinds PW. 2001. The retinoblastoma protein acts as a transcriptional coactivator required for osteogenic differentiation. Mol Cell 8:303–316.

Vaes BL, Ducy P, Sijbers AM, Hendriks JM, van Someren EP, de Jong NG, van den Heuvel ER, Olijve W, van Zoelen EJ, Dechering KJ. 2006. Microarray analysis on Runx2-deficient mouse embryos reveals novel Runx2 functions and target genes during intramembranous and endochondral bone formation. Bone 39:724–738.

Vaughan T, Pasco JA, Kotowicz MA, Nicholson GC, Morrison NA. 2002. Alleles of RUNX2/CBFA1 gene are associated with differences in bone mineral density and risk of fracture. J Bone Miner Res 17:1527–1534.

Vaughan T, Reid DM, Morrison NA, Ralston SH. 2004. RUNX2 alleles associated with BMD in Scottish women; interaction of RUNX2 alleles with menopausal status and body mass index. Bone 34:1029–1036.

Vega RB, Matsuda K, Oh J, Barbosa AC, Yang X, Meadows E, McAnally J, Pomajzl C, Shelton JM, Richardson JA, Karsenty G, Olson EN. 2004. Histone deacetylase 4 controls chondrocyte hypertrophy during skeletogenesis. Cell 119:555–566.

Wang W, Wang YG, Reginato AM, Glotzer DJ, Fukai N, Plotkina S, Karsenty G, Olsen BR. 2004. Groucho homologue Grg5 interacts with the transcription factor Runx2-Cbfa1 and modulates its activity during postnatal growth in mice. Dev Biol 270:364–381.

Wei CL, Wu Q, Vega VB, Chiu KP, Ng P, Zhang T, Shahab A, Yong HC, Fu Y, Weng Z, Liu J, Zhao XD, Chew JL, Lee YL, Kuznetsov VA, Sung WK, Miller LD, Lim B, Liu ET, Yu Q, Ng HH, Ruan Y. 2006. A global map of p53 transcription-factor binding sites in the human genome. Cell 124:207–219.

Weinmann AS, Bartley SM, Zhang T, Zhang MQ, Farnham PJ. 2001. Use of chromatin immunoprecipitation to clone novel E2F target promoters. Mol Cell Biol 21:6820–6832.

Westendorf JJ. 2006. Transcriptional co-repressors of Runx2. J Cell Biochem 98:54–64.

Wiley SR, Winkles JA. 2003. TWEAK, a member of the TNF superfamily, is a multifunctional cytokine that binds the TweakR/Fn14 receptor. Cytokine Growth Factor Rev 14:241–249.

Xiao ZS, Hinson TK, Quarles LD. 1999. Cbfa1 isoform overexpression upregulates osteocalcin gene expression in non-osteoblastic and pre-osteoblastic cells. J Cell Biochem 74:596–605.

Xiao G, Jiang D, Gopalakrishnan R, Franceschi RT. 2002. Fibroblast growth factor 2 induction of the osteocalcin gene requires MAPK activity and phosphorylation of the osteoblast transcription factor, Cbfa1/Runx2. J Biol Chem 277:36181–36187.

Yoshida CA, Furuichi T, Fujita T, Fukuyama R, Kanatani N, Kobayashi S, Satake M, Takada K, Komori T. 2002. Core-binding factor beta interacts with Runx2 and is required for skeletal development. Nat Genet 32:633–638.

Zaidi SK, Sullivan AJ, Medina R, Ito Y, van Wijnen AJ, Stein JL, Lian JB, Stein GS. 2004. Tyrosine phosphorylation controls Runx2-mediated subnuclear targeting of YAP to repress transcription. EMBO J 23: 790–799.

Zhang YW, Yasui N, Ito K, Huang G, Fujii M, Hanai J, Nogami H, Ochi T, Miyazono K, Ito Y. 2000. A RUNX2/PEBP2alpha A/CBFA1 mutation displaying impaired transactivation and Smad interaction in cleidocranial dysplasia. Proc Natl Acad Sci USA 97:10549–10554.